Journal of Contemporary Issues in Business and Government Vol. 25, No. 01, 2019
https://cibgp.com/

P-ISSN: 2204-1990; E-ISSN: 1323-6903
DOI: 10.47750/cibg.2019.25.01.029

HOMOTOPY OPTIMIZATION FOR THE COMPRESSION OF A MULTIBODY MODEL OF A VEHICLE

BANTU SAILESH 1, PRAVEEN KUMAR MUNNANGI2,
ASSOCIATE PROFESSOR 1, ASSISTANT PROFESSOR 2,
Mail ID: sailesh.bantu04@gmail.com, Mail ID:praveenmunnangi009@gmail.com
Dept.: Mechanical
Pallavi Engineering College,
Kuntloor(V),Hayathnagar(M),Hyderabad,R.R.Dist.-501505.

abstract

For tasks like design optimization, sensitivity analysis, parameter identification, and controller tuning, which can require hundreds or thousands of simulations, the reduction of complex multibody dynamic models remains an important topic of investigation, despite the increasing computational power of modern processors. Initially, we create a detailed Adams/Car model of a mass-produced SUV. Then, in Maples, we create front and rear suspension models called single-link equivalent kinematic quarter-cars (SLEKQ, pronounced "sleek"). All suspension connections are combined into one unsprung mass at each corner of the vehicle to reduce the computational complexity of including bush ings or kinematic loops. The high-fidelity Adams model is used to generate lookup tables or polynomial functions that are then used in the SLEKQ models to simulate the kinematic behaviour of a complete suspension model. Each SLEKQ model's capacity to forecast behaviour is contingent on the accuracy with which its nonlinear spring and damper parameters, such as the bushings' stiffness and damping contributions and the unsprung mass, are accounted for. Parameters that allow for the smallest gap between Adams and MapleSim model responses are found through homotropy optimization. Four-post heave and pitch tests are used to verify the dynamic performance of the SLEKQ models integrated into a reduced 10-degree-of-freedom model of the whole vehicle compared to the high-fidelity Adams model.

production

The methodical development of a minimum complicated model that describes the behaviour of interest in the original model with enough accuracy is a central goal of model reduction approaches [1]. This goal is similar to Einstein's famous remark that models should be made as simple as feasible, but no simpler [2]. Particularly in the design and optimization of car suspensions, where bushings and kinematic loops lead to stiff or differential-algebraic equations that may be time-consuming to solve, a simplified model can be of great assistance. First, we create detailed Adams/Car1 models of a production SUV's front MacPherson strut and rear semi-trailing-arm multi-link suspensions. Then, we use MapleSim2 to create a model of a quarter-car with a single equivalent kinematic link (SLEKQ, pronounced "sleek"). Suspension links are treated as a single un sprung mass at each corner of the car, similar to the method employed by Charism [3], to reduce the computing complexity of the model and account for things like bushings and kinematic loops. Each SLEKQ model has the same kinematic behaviour as the comparable full sus pension model, which is a significant improvement over the simplistic quarter-car models that have been utilized before and give merely approximations of the genuine suspension kinematics. The kinematic behaviour of each SLEKQ model is defined in this study using polynomial functions acquired from the high-fidelity Adams model. A benefit of this method is that it allows a single multibody model to be used to represent a wide variety of suspension types by simply modifying the kinematic curves and model parameters. Furthermore, rather than revising particular hard point localtons, the performance implications of shifting the suspension curves (such as the connection between camber and vertical displacement) may be examined simply by tweaking these curves directly in the model.

Each SLEKQ model's dynamic performance is dependent on the precision of the parameters chosen for the nonlinear spring and damper (which includes the stiffness and damping contributions of the bushings) and the unsprung mass. Homotropy optimization [4], an optimization method that aims to prevent convergence to a local minimum, is used to determine the parameters that minimize the difference between the Adams model's response and the Maples model's response. This study employs homotropy optimization in a manner similar to that provided by Vyasarayani et al. [6], and is connected to the work of Abarbanel et al. [5]. After determining the appropriate values for the SLEKQ models' characteristics, a simplified, 10-DOF model of the whole vehicle is built and compared to the Adams model in terms of its

P-ISSN: 2204-1990; E-ISSN: 1323-6903
DOI: 10.47750/cibg.2019.25.01.029

dynamic performance. In Section 2, we get a quick rundown of how the high-fidelity Adams model came to be. In Section 3 we detail the steps used to create the SLEKQ model. Parameter optimization for the simplified model is discussed in Section 4, and Section 5 presents and verifies the resulting identification of the model's parameters. In Section 6, we provide our last thoughts and plans for further development.

Detailed representation of the Adams atmosphere

Adams/Car 2010, a software package often used in the automotive industry for simulating vehicle dynamics, is used to first construct a high-quality complete vehicle model to help in the creation and tweaking of the reduced model. Specs and measurements from component drawings are used to refine the model. As can be seen in Figure 1, the production SUV under investigation rides on a MacPherson strut up front and a semi-trailing arm multi-link setup in the back.

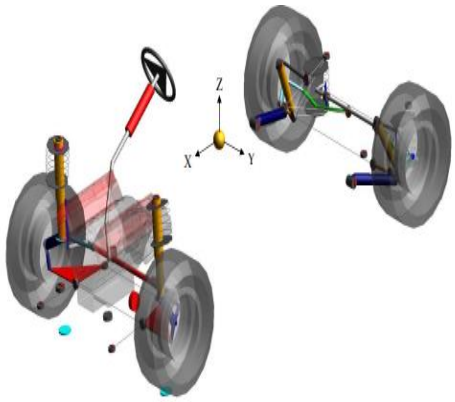

Detailed representation of the Adams/Car model fig.1

Linear rates for the suspension coil springs and splines characterizing the response of the dampers are calculated based on data from the component specifications. Per [7], bushings are modeled as linear components with damping rates equal to 1% of the linear stiffness rates. Other chassis parts like control arms, uprights, and subframes are all modeled as rigid bodies with known masses and estimated inertias based on material characteristics and approximations of component geometry.

Kinematic equivalent of a quarter-car based on a single connection

MapleSim 5 implements a simplified version of the Adams model presented in Section 2. The high-fidelity model's suspension is replaced with a simplified model using a massless suspension joint, which is aimed to maintain the same kinematic performance as the high-fidelity model (using data gained from Adams) while removing all closed kinematic chains. To create a scaled-down version of the vehicle, the SLEKQ models' specifications are first determined. MapleS symbolic m's simplification and optimization methods provide computationally efficient, dynamic simulation code, which is especially useful for parameter discovery. For sensitivity analysis, the symbolic expressions' capacity to be differentiated might be helpful as well. The unsprung mass's orientation (as a function of camber, caster, and toe), as well as its X and Y displacements, as a function of its vertical displacement, may be calculated with the use of lookup tables or polynomial functions generated using the Adams model. There is usage of polynomials of the second and third orders in this work. The geometry of the suspension may be used to derive these kinematic suspension curves experimentally or, in simple circumstances, mathematically. The suspension toe angle (around the Z-axis) and camber angle establish the first two of three body-fixed rotations needed to determine the orientation of the unsprung mass (about the rotated X 0 -axis). Although the heave motion of the suspension may be linked to a change in the steering axis, the steering axis definition varies across suspension types, making it impossible to create a universal function that relates the third revolution (around the Y00-axis) to the steering axis's orientation. For the validation of the rotational kinematics of the SLEKQ model (see Figure 2), MapleSim reports the orientation of a rigid body using 9 direction cosines; for the validation of the translational kinematics, it is a simple matter to compare the two sets of data.

After the SLEKQ model's kinematic behaviour has been verified, its dynamic behaviour may be taken into account. Finding the spring and damper's base in a coordinate system that is fixed with respect to the unsprung mass is the first step. If you want the forces created by your spring and damper to be applied in the right direction, you need to make

P-ISSN: 2204-1990; E-ISSN: 1323-6903
DOI: 10.47750/cibg.2019.25.01.029

sure their bases are in the right places. It is also necessary to calculate the spring stiffness and damping coefficients of efficiency. As this effort aims to construct a simpler, computationally efficient model, it does not represent the bushings separately. Instead, it is necessary to identify the spring and damper curves, which include the bushing's stiffness and damping effects. The

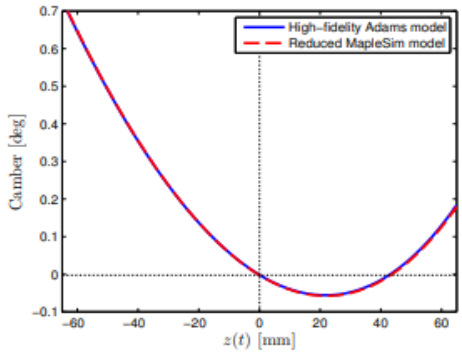

Verification of front camber, shown in Fig.2 An analytical method for determining how much each bushing in the SLEKQ model affects the overall system behaviour would be prohibitively time-consuming and inaccurate, making this a perfect chance to use a parameter identification technique. The damping force is specified by the following piecewise linear function:

$$F_d(t) = \begin{cases} -d_1 d_2 - d_3(v(t) + d_2), & v(t) < -d_2 \\ -d_1 v(t), & -d_2 \le v(t) < 0 \\ -d_4 v(t), & 0 \le v(t) < d_5 \\ -d_4 d_5 - d_6(v(t) - d_5), & v(t) \ge d_5 \end{cases}$$

where v(t) is the velocity of the damper piston, d1 and d4 are the low-speed bump and rebound rates, d2 and d5 define the speeds at which the low- and high-speed bump and rebound transition, and d3 and d6 are the high-speed bump and rebound rates. Parameter identicfiction is used to calculate all of the coefficients d. The selection of Equation 1 was based on its flexibility to include bump and rebound damping variances, as well as low and high-speed damping differences. For the sake of C 1 continuity, note that a Bezier curve of second order is employed at each transition in Equation 1. Here's how we pin down the meaning of spring force:

$$F_k(t) = k_3 \Delta L^3 + k_2 \Delta L^2 + k_1 \Delta L + k_0$$

where L is the compression of the spring relative to its original length and ki is a set of coefficients. It was determined that a polynomial of degree 3 was a close enough approximation of the spring curve to be useful. The unsprung mass is the last unknown in the SLEKQ model. Unsprung mass is made up completely of the upright and everything outside of it; how much of each control arm and drive shaft is sprung or unsprung is unclear. The automobile industry is known for using different approximations, such as dividing the total mass of these parts evenly between the sprung and unsprung masses [8]. However, the unsprung mass is also determined to increase the precision of the simplified model.

Locating Critical Parameters

Parameter identification in a mathematical model may be thought of as an optimization issue in which the goal is to minimize the difference between the experimental data and the predicted result of the model [9]. The homotropy optimization approach [4] was chosen because it can maintain convergence to a global minimum even when only mediocre initial parameter estimations are available (as is the case in this work). In addition, parameter identification issues for reduced vehicle models [6] and other multibody systems [10] have been effectively used to homotropy optimization with positive results. Coupling a high-gain observer to the motion equations is an essential part of the homotropy optimization strategy [11]:

$$\dot{\mathbf{x}} = \mathbf{f}(\mathbf{x}, \mathbf{p}, t) + \lambda \mathbf{\Gamma} \mathbf{e}(t)$$

where x is the state vector, p is the vector of unknown parameters, is the vector of observer gains, and e(t) is the vector of time-varying errors (the difference between the experimental data and the model response). Convergence to a local minimum is avoided because of the observer term e(t), which smooths the objective function. Initially, the observers are completely linked to the equations of motion (= 1), which is the starting point for the parameter identification procedure. When = 1, the gains must be large enough to make the mathematical model match the experimental data. The method gradually decreases, bringing the coupling term down to a more manageable size. Then, the ideal parameter values from the previous step are used as starting points for optimizing the parameters p. This procedure is repeated until = 0,

P-ISSN: 2204-1990; E-ISSN: 1323-6903
DOI: 10.47750/cibg.2019.25.01.029

at which point the original equations of motion are reconstructed. If is small enough, the method will provide initial parameter estimations that are near to the global optimum, preventing it from falling into a local minimum [6]. Figure 3 is a simplified version of the quarter-car model we'll use to illustrate how homotropy optimization may be used to determine appropriate values for a given set of parameters. Next, we will see how the same approach may be used with a nonlinear SLEKQ model in Section 5. In a kinematics and compliance test, the unsprung mass munsp and spring and damper behaviour are determined by anchoring the sprung mass msp to the ground and applying a vertical force FZ (t) at the tire contact patch. We'll use an assumption to cut down on the complexity of this talk.

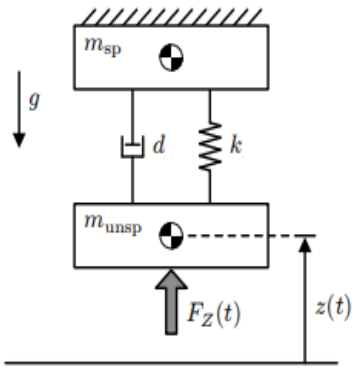

An example of a linear mass-spring-damper system is shown in Figure 3.

In Maples mod ell, Equations 1 and 2 explain the linear behaviour of the damper and the spring. This system of mass, spring, and damper is described by the following ordinary differential equation of the second order:

$$m_{\text{unsp}}\ddot{z}(t) = F_Z(t) - d\dot{z}(t) - kz(t) - m_{\text{unsp}}g$$

in which the damping and stiffness coefficients, d and k, respectively. Equation 4 is updated to include the homotropy coupling term on the right-hand side. The forcing term is a PID controller that takes the form of an error in location, velocity, and acceleration.

$$\lambda\left\{G_I N_I(z_e(t) - z(t)) + G_P N_P(\dot{z}_e(t) - \dot{z}(t)) + G_D N_D(\ddot{z}_e(t) - \ddot{z}(t))\right\}$$

where NI, NP, and ND are used to normalize the errors and Ze(t), Ze(t), and Ze(t) are the experimental location, velocity, and ac celebration data we desire to monitor using Equation 4. For the mathematical model to accurately reproduce the experimental data when = 1, the correct PID gains GP, GI, and GD must be found. Figure 4 depicts the homotropy coupling term as it is implemented in Maples. Matlab3 is used for the parameter identification process once the final Maples model has been exported as an S-function. The objective function is minimized for each value of using the mesarch routine [12], which is based on the Nelder-Mead simplex approach.

$$J = w_1 \int_0^{t_f} (z_e(t) - z(t))^2 dt + w_2 \int_0^{t_f} (\dot{z}_e(t) - \dot{z}(t))^2 dt + w_3 \int_0^{t_f} (\ddot{z}_e(t) - \ddot{z}(t))^2 dt$$

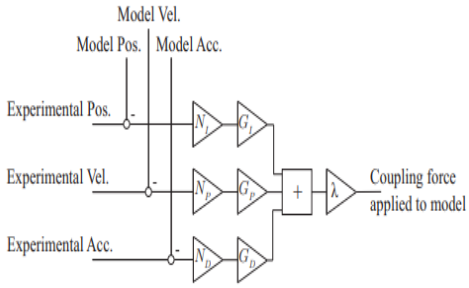

As shown in Fig. 4, the homotropy coupling term has been implemented in Maples.

where the weights wi are used to calculate z(t), z(t), and z(t) from Equations 4 and 5. Using a swept-sine force input FZ (t) = F0 + 1.0 sin(t) kN, where F0 is the corner weight of the vehicle, the high-fidelity Adams model generates experimental data. It is recommended that the input signal have a frequency range of 0 Hz to 6 Hz [13] to accurately represent the suspension behaviour seen during normal freeway driving. To ensure that the smaller Maples model has the same ride height as the Adams model, the undeformed length of the spring is calculated. Milliken and Milliken [8] provide a technique to estimating mumps in which the sprung and unsprung masses of suspension parts are divided evenly. Using the Adams model's information on ride rates, a rough approximation of the spring curve may be made. To begin with, we just use the damper from the Adams model to estimate the damper curve since we don't know how much of an effect the bushings have on the damping properties of the suspension.

Critical Discussion and Outcomes

Parameters for two SLEKQ models are identified using the homotropy optimization strategy outlined in Section 4. One model represents the front suspension of the high-fidelity model, while the

P-ISSN: 2204-1990; E-ISSN: 1323-6903
DOI: 10.47750/cibg.2019.25.01.029

other represents the rear suspension. Figures 5 and 6 show the models' responses with the initial parameter estimates and the final identified parameters, while Table 1 lists the homotropy coupling gains used by each model. Take note that the forward SLEKQ model more closely follows the experimental data than the backward one. Two characteristics of the rear suspension not captured by the current SLEKQ model are to blame for this disparity. Specifically, as can be seen in Figure 1, the rear damper is not quite as vertical as the front. Moreover, the back

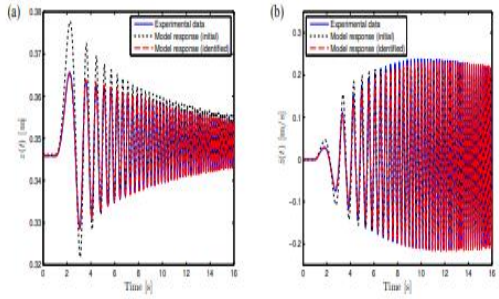

Figure 5: (a) displacement and (b) unsprung mass velocity compared to experimental data and model response for front suspension using initial parameter estimations.

Gains in homotropy coupling that were used to achieve optimal performance for each SLEKQ model are listed in Table 1.

	G_I	G_P	G_D
Front suspension	0.1	2.0	1.0
Rear suspension	0.5	1.5	0.8

There is a soft bushing connecting the damper to the chassis. This combination of characteristics causes a substantial longitudinal component in the damper force at high piston velocities, which in turn deforms the comparatively soft bushing at the damper-to-chassis mount, significantly altering the system's response. Figure 6 shows that at higher frequencies, the experimental data and model response diverge, indicating that while the damping curve has been discovered, the phenomena cannot be recreated exactly.

Table 2 demonstrates that the measured unsprung masses for both the front and rear suspensions fall within physically acceptable limits (i.e., between 0% and 100% of the mass of the suspension links).

A list of identified parameters for unsprung masses is shown in Table 2.

	Lower bound [kg]	Upper bound [kg]	Initial guess [kg]	Identified value [kg]
Front suspension	58.5	63.7	61.1	59.1
Rear suspension	63.9	76.1	70.0	64.1

In both circumstances, the suspension links account for a significant portion of the mass that is sprung. Figure 7 depicts determined spring curves for both the front and rear suspensions, showcasing springs that are just slightly stiffer than those utilized in the Adams high-fidelity model.

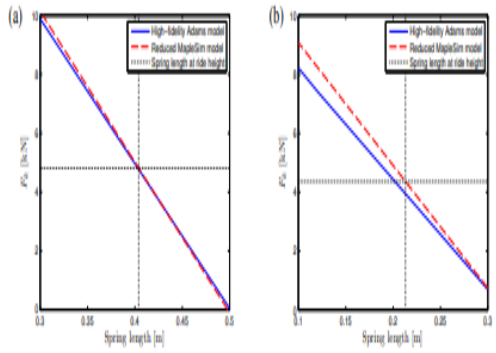

Fig. 7. Force-displacement curves for springs in Adams and Maples models on (a) front and (b) rear suspensions

The identified damper curves are shown in Figure

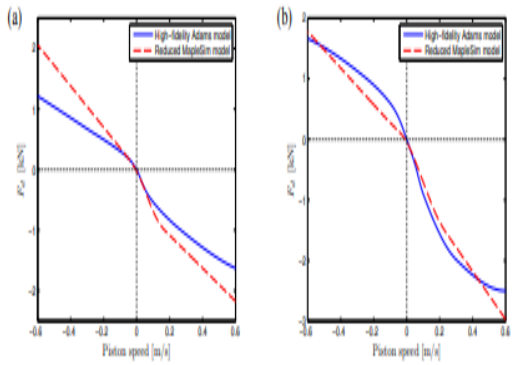

Figure 8: (a) front and (b) rear suspension force-velocity curves from the Adams and MapleSim models, respectively.

The identification process has the same effect in both circumstances, making the damper more rigid at high speeds. The bump damping (negative damper piston speed) of both the front and rear suspensions is essentially linear.

P-ISSN: 2204-1990; E-ISSN: 1323-6903
DOI: 10.47750/cibg.2019.25.01.029

The front and rear sus pensions are used to construct a comprehensive vehicle model for four-post testing, validating the parameter identification findings in the process. The vehicle's sprung mass is represented by a single rigid body to which four SLEKQ models are linked. It is expected that the existing model is symmetrical in a horizontal plane. Since only the heave and pitch movements are being studied at the moment, the only other parameters in the four-post model are the wheelbase, the position of the center of gravity of the sprung mass, and the mass and pitch inertia of the sprung mass. All of these extra characteristics come straight from the high fidelity model. For the heave test, the front and rear suspensions are excited in phase, whereas for the pitch test, the front and rear suspensions are excited 180 degrees out of phase. Both use a sinusoidal sweep with a constant velocity of 30 mm/s and a frequency range of 0 to 6 Hz. These assessments are run once more on the Adams high-fidelity model for the sake of comparison. Figure 9 displays the findings, which verify that correct parameters have been determined for the SLEKQ models.

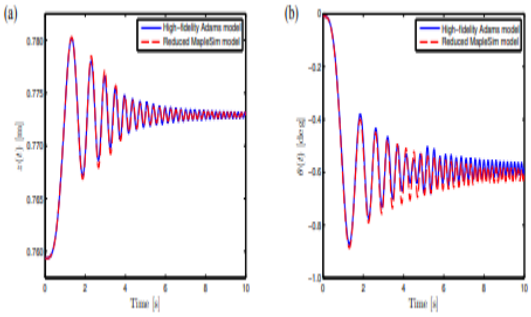

Figure 9: (a) vertical chassis displacement during the heave test, and (b) chassis pitch during the pitch test, both from four-post validation testing.

Results and Future Directions

A massless suspension joint was used in the building of a MapleSim model of a quarter-car with an analogous kinematic single-link suspension. This model's response is identical to that of a MacPherson strut front suspension modeled in Adams/Car by using homotopy optimization to determine the unsprung mass and coefficients for the spring and damper curves. It has been shown that the simplified model is flexible enough to be utilized to simulate the reaction of a semi-trailing-arm multi-link rear suspension. Using these simplified suspension models, we constructed a whole car dummy and put it through four-post testing to verify the results. Rear suspension's relatively soft bushing between the damper and chassis calls for more research into how compliance might be included into the simplified form. We will also look at the chassis's rigidity and whether or not the vehicle's assumed lateral symmetry holds water. The chassis's roll and yaw inertias, as well as its track widths, will be determined by conducting roll and warp four-post tests.

REFERENCES

[1] Wilson B.H., Stein J. L.: An algorithm for obtaining proper models of distributed and discrete systems, ASME Journal of Dynamic Systems, Measurement, and Control, 117 (4), 534-540, 1995.

[2] Einstein A.: On the method of theoretical physics, Philosophy of Science, 1 (2), 163-169, 1934.

[3] Sayers M.W.: Vehicle models for RTS applications, Vehicle System Dynamics, 32 (4-5), 421-438, 1999.

[4] Watson L.T.: Globally convergent homotropy algorithms for nonlinear systems of equations, Nonlinear Dynamics, 1 (2), 143-191, 1990.

[5] Abarbanel H.D.I., Creveling D.R., Farsian R., Kostuk M.: Dynamical state and parameter estimation, SIAM Journal on Applied Dynamical Systems, 8 (4), 1341-1381, 2009.

[6] Vyasarayani C.P., Uchida T., Carvalho A., McPhee J.: Parameter identification in dynamic systems using the homotopy optimization approach, Multibody System Dynamics, 26 (4), 411-424, 2011.

[7] Mechanical Dynamics Inc., ADAMS/Pre 11.0 Reference Guide, 2001.

[8] Milliken W.F., Milliken D.L.: Race Car Vehicle Dynamics, Society of Automotive Engineers, Warrendale, 1995.

[9] Serban R., Freeman J.S.: Identification and identifiability of unknown parameters in multibody dynamic systems, Multibody System Dynamics, 5 (4), 335-350, 2001.

[10] Vyasarayani C.P., Uchida T., McPhee J.: Nonlinear parameter identification in multibody systems using homotopy continuation, ASME Journal of Computational and Nonlinear Dynamics, 7 (1), 011012, 2012.

[11] Khalil H.K.: High-gain observers in nonlinear feedback control, H. Nijmeijer and T. I. Fossen, New Directions in Nonlinear Observer Design, Lecture Notes in Control and Information Sciences, 244, Springer, 249-268, 1999.

[12] Lagarias J.C., Reeds J.A., Wright M.H., Wright P.E.: Convergence properties of the Nelder– Mead simplex method in low dimensions, SIAM Journal on Optimization, 9 (1), 112-147, 1998.

[13] Gillespie T.D.: Fundamentals of Vehicle Dynamics, Society of Automotive Engineers, Warrendale, 1992.